

Supporting information

Enhanced thermoelectric properties of SnSe thin films grown by single-target magnetron sputtering

Lirong Song,^a Jiawei Zhang,^a and Bo Brummerstedt Iversen^{a,*}

^a Center for Materials Crystallography, Department of Chemistry and iNANO, Aarhus University, DK-8000 Aarhus, Denmark.

*E-mail: bo@chem.au.dk

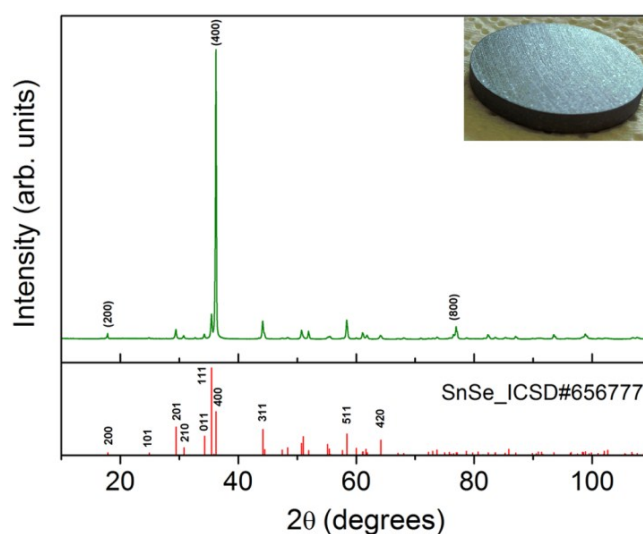


Fig. S1 XRD pattern of SnSe sputtering target (Co K α radiation, $\lambda = 1.79 \text{ \AA}$). The inset shows the picture of the as-synthesized SnSe target.

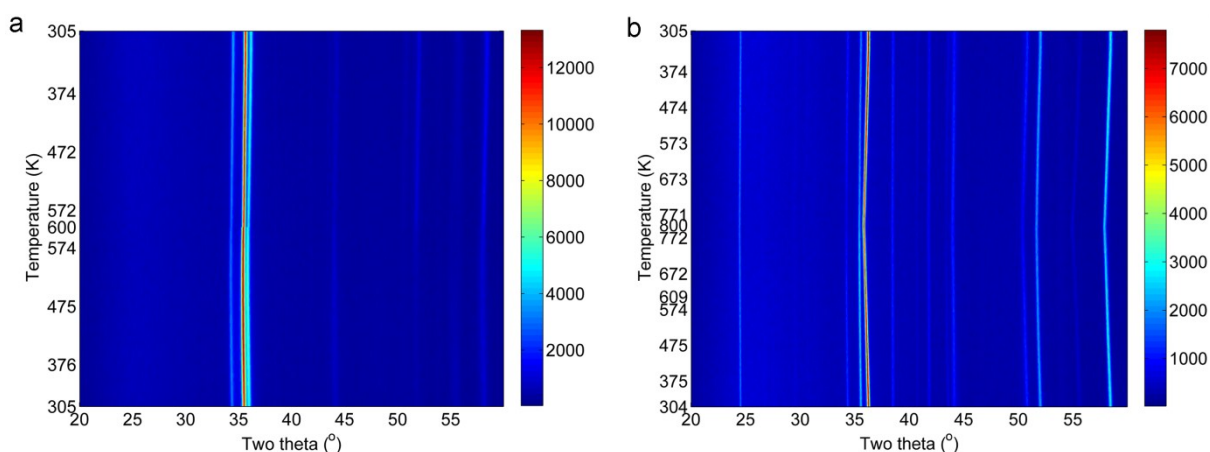


Fig. S2 In-house *in situ* XRD patterns using contour plot for the annealed thin film samples (a) ss_600 and (b) ss_800.

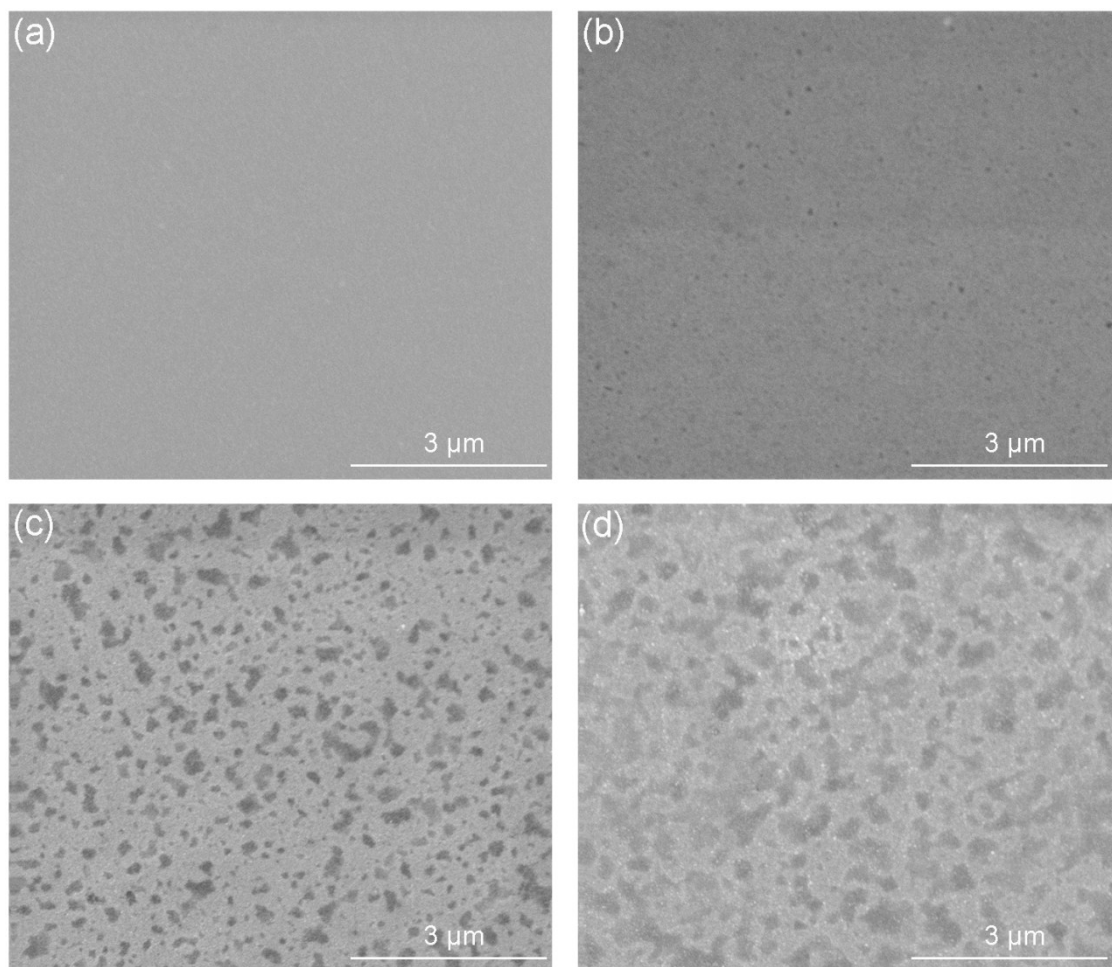


Fig. S3 SEM images of the surfaces of the annealed SnSe thin film samples (a) ss_600, (b) ss_700, (c) ss_800, and (d) ss_1000.

Table S1 Actual compositions of the as-deposited thin film measured by SEM-EDS.

Measured regions	Sn (at.%)	Se (at.%)
#1	52.23	47.77
#2	52.66	47.34
#3	52.19	47.81
#4	52.19	47.81
#5	52.30	47.70
#6	52.08	47.92
Average	52.275	47.725

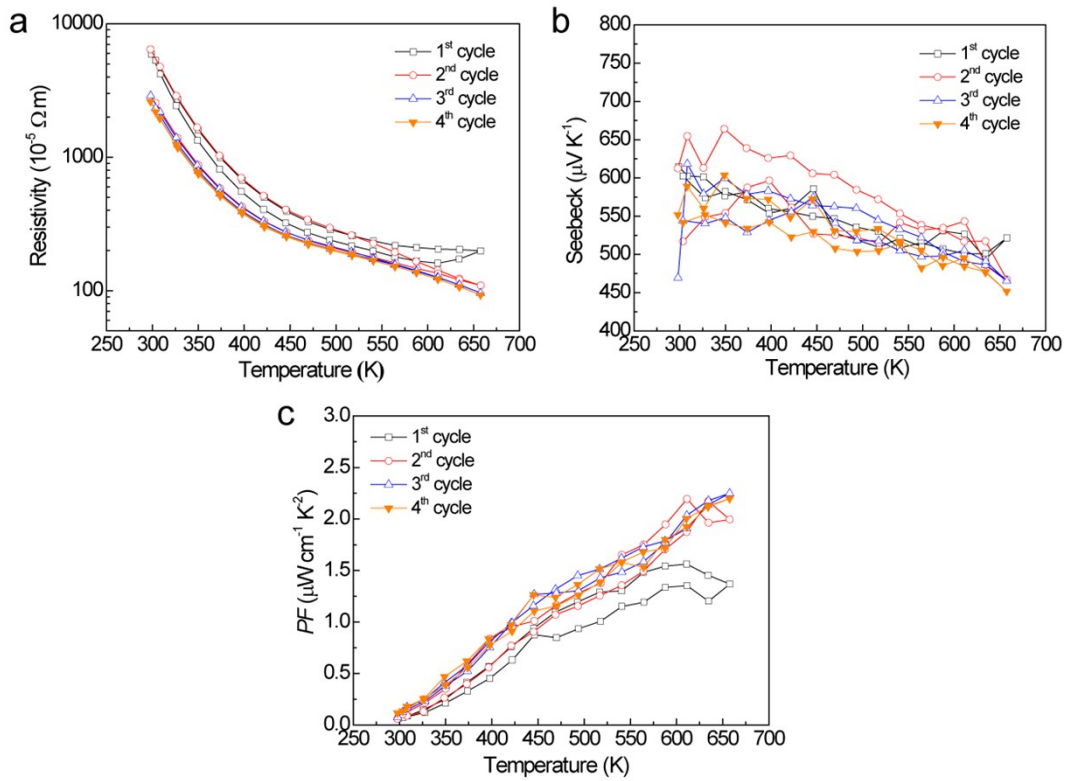


Fig. S4 Temperature-dependent thermoelectric properties: (a) electrical resistivity, (b) Seebeck coefficient and (c) power factor in four cycles of both heating and cooling for the annealed thin film sample (ss_700).

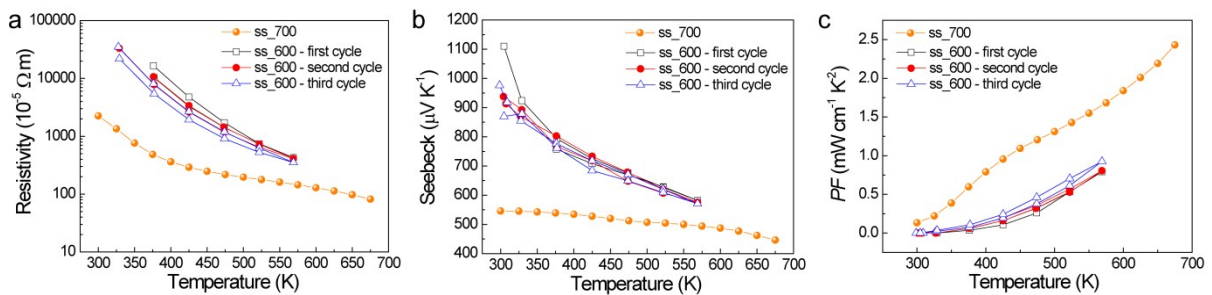


Fig. S5 Temperature-dependent thermoelectric properties: (a) electrical resistivity, (b) Seebeck coefficient and (c) power factor for the annealed thin film sample (ss_600) in comparison with the annealed thin film sample (ss_700).

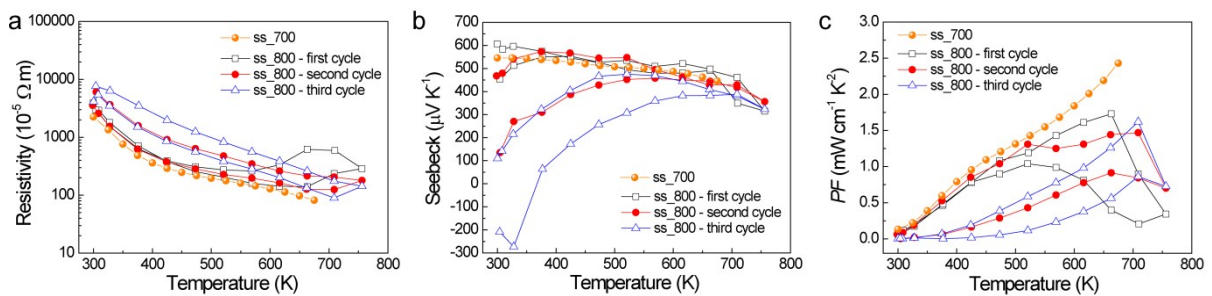


Fig. S6 Temperature-dependent thermoelectric properties: (a) electrical resistivity, (b) Seebeck coefficient and (c) power factor for the annealed thin film sample (ss_800) in comparison with the annealed thin film sample (ss_700).

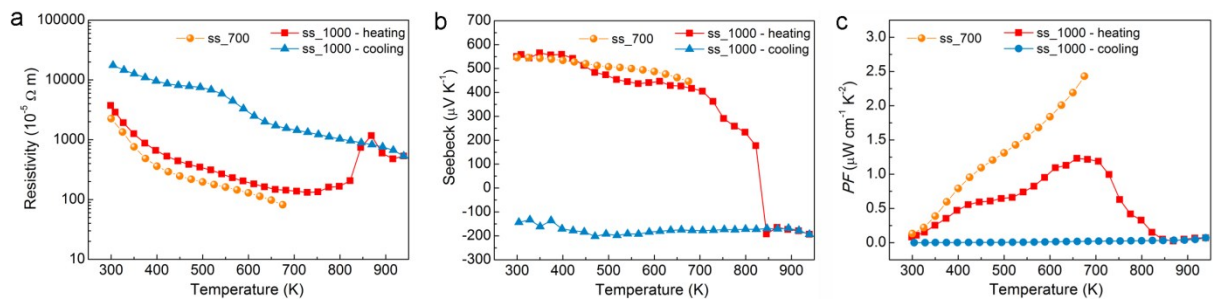


Fig. S7 Temperature-dependent thermoelectric properties: (a) electrical resistivity, (b) Seebeck coefficient and (c) power factor for the annealed thin film sample (ss_1000) in comparison with the annealed thin film sample (ss_700).